Nonlinear oscillations of ultra-cold atomic clouds in a magneto-optical trap

Luiz Gustavo Ferreira Soares and Fernando Haas

Instituto de Física, Universidade Federal do Rio Grande do Sul,

Av. Bento Gonçalves 9500, 91501-970 Porto Alegre, RS, Brasil

Abstract

Confined atomic clouds in a magneto-optical trap can be formally interpreted as a single component trapped plasma. An hydrodynamical model in a three-dimensional geometry with radial symmetry is applied. A general polytropic equation of state is assumed. For suitable initial conditions and velocity fields, the Lagrangian variables method reduces the problem to ordinary differential equations in the limiting cases according to the prevalence of thermal or multiple-scattering effects. The thermal, pressure dominated case with adiabatic equation of state leads to a dissipative nonlinear oscillator with an inverse cubic force, in the form of a damped Pinney equation. An accurate approximate analytic solution derived from Kuzmak-Luke perturbation theory allows the assessment of the fully nonlinear dynamics. The applicability conditions of the two regimes are discussed. The intermediate case where both thermal and multiple-scattering effects are equally relevant is also analytically studied.

PACS numbers: 02.30.Hq, 05.70.Ce, 37.10.Gh, 47.10.Fg, 51.30.+i

Keywords: trapped cold atoms, exact nonlinear oscillations, Lagrangian variables, Pinney equation, temperature limited conditions, magneto-optical trap, multiple-scattering regime.

I. Introduction

Among the most successful techniques to produce large samples of optically confined cold atoms are the magneto-optical traps (MOTs), which consist of the intersection of three pairs of orthogonal oppositely circularly polarized beams with a spatially varying magnetic field [1, 2]. Such confinements involve the joint effects of the magnetic trapping and the Doppler cooling mechanisms [3, 4]. MOTs are essential in the realization of optical lattices [5, 6], Bose-Einstein condensates [7], observation of collective quantum effects [8] and in atomic clocks performance enhancement [9, 10]. The dynamics of cold trapped gases in a MOT share many similarities with confined non-neutral plasmas such as an antiproton gas in a Penning-Malmberg trap cooled to extremely low temperatures [11] and a closer analogy with astrophysical models for pulsating stars [4, 12]. The optical cooling and trapping of highly magnetic atoms [13], the self-induced electron trapping in freely expanding ultra-cold plasmas [14] and the coherent excitation of Rydberg states in cold atomic gases [15] also show the timeliness and a broad interest on complex phenomena in MOTs. Previous studies rely on linear approximation [16–18] or purely numerical [19] analysis. In the stationary case, a first analytical attempt was made by means of a Taylor series technique [20]. Here we provide an alternative solution method allowing the assessment of the nonlinear and time-dependent dynamics, using Lagrangian variables.

At the low saturation regime, a confined atomic cloud in a MOT can be formally interpreted as a single component trapped plasma, corresponding to an effective weak charge $q_{eff} \sim 10^{-4}e$ to $10^{-6}e$, where e is the elementary charge [21]. Such similarities makes possible to apply to MOTs well known hydrodynamical models from plasma physics [16–18]. In this context, we will consider nonlinear time-dependent structures derived by means of the Lagrangian coordinates method [22–24]. Lagrangian variables are recognized as effective in fluid problems and have been recently applied e.g. for the derivation of nonlinear waves in one-dimensional degenerate electron gases [25] and large amplitudes oscillations of single component trapped plasma with collisional drag [26]. Hence we transform from Eulerian variables to comoving fluid coordinates.

In the hydrodynamic model, the repulsive collective force and the pressure term tend to produce expansion, while an external gradient field provides harmonic confinement. Due to the Doppler cooling, the model also has a damping term. Experiments with MOTs are usually performed in the temperature-limited (TL) regime or in the the multiple-scattering (MS) regime, that dominates the long range interactions. These cases depend upon the number of confined atoms. Measurements of the angular frequency, damping coefficient, temperature and size of the cloud have been made with trapped cesium and rubidium in both situations [1, 27–32]. Achieving the TL regime is an important step towards the observation of collective quantum effects, since in the MS regime the number density remains invariant under addition of atoms [3].

In this context two basic situations will be considered, according to the prevalence of thermal effects (for lower densities) or long range interactions (for higher densities). The precise conditions for the two limiting cases have to be evaluated in terms of the physical parameters. However, in an intermediate case between the isothermal and adiabatic regimes, analytical conclusions are also accessible in the mixed TL + MS situation, as described in II.C. As remarked in [20], it is appropriate to consider MOT confinements under diverse equations of state. Therefore, we assume a general polytropic equation of state, which is useful for most experimental setups. Our treatment is restricted to traps with perfectly aligned lasers so that we will consider systems with radial symmetry. However, the method can be advanced for stable structures with misalignment in the xy-plane [31, 33].

This work is organized as follows. Section II introduces the basic set of hydrodynamic equations and the transformation to Lagrangian variables. Accordingly, in II.A we develop the full solution when thermal effects are dominant over the multiple-scattering effects and provides the precise applicability conditions of the solution in terms of the relevant physical parameters. In II.B we perform the same treatment in the opposite case of the MS regime, while in II.C the intermediate regime is developed. Section III discuss the conditions for applicability of the diverse solutions. Section IV is reserved to the conclusions.

II. Basic model and Lagrangian variables method

In a three-dimensional geometry with radial symmetry, the dynamics of a cold trapped gas in a MOT can be described by the following hydrodynamic equations

$$\frac{\partial n}{\partial t} + \frac{1}{r^2}\frac{\partial}{\partial r}(r^2 n v) = 0\,, \tag{1}$$

$$\frac{\partial v}{\partial t} + v\frac{\partial v}{\partial r} = -\frac{1}{mn}\frac{\partial P}{\partial r} - \omega^2 r - \nu v + \frac{F_c}{m}\,, \tag{2}$$

$$\frac{1}{r^2}\frac{\partial}{\partial r}(r^2 F_c) = Qn\,, \tag{3}$$

where Eqs. (1-3) are respectively continuity, momentum and Gauss law equations. By definiteness, the system is composed by cold atoms (atomic mass m) with a number density n, fluid velocity with radial component v and pressure P. The simplest model to describe the MOT force, which originate from the Zeeman shift and the Doppler cooling, is the Doppler model at low saturation limit, which is given when the incident on-resonance saturation parameter per beam $s_{inc} << 1$. This parameter describes the ratio between the incident lasers intensities and their saturation value. In this context, the average forces acting on a single moving atom are based on the quasi-resonant radiation pressure which, due the gradient magnetic field and the three pairs of beams, can be described, respectively, as an harmonic force with angular frequency ω and a dissipative force with damping coefficient ν. For that reason, the confinement is provided by the Zeeman shift and the damping force by the Doppler cooling. In this model, assuming symmetric forces [16–18, 20],

$$\nu = -\frac{8\hbar k_L^2 s_{\rm inc}\Delta}{m\Gamma(1+4\Delta^2/\Gamma^2)^2}, \quad \omega = (\nu\mu/k_L)^{\frac{1}{2}}\,, \tag{4}$$

where k_L is the amplitude of the laser wave vector, $\hbar$ is the reduced Planck constant, Δ is the frequency detuning between the laser frequency and the atomic transition frequency and Γ is the natural line width of the transition used in the cooling process. Also, $\mu = \mu_B|\nabla B|/\hbar$, with μ_B being the Bohr magneton and $|\nabla B|$ the intensity of the gradient field, assumed to be symmetric in all directions. In MOTs the red detuning ($\Delta < 0$) is used, so that $\nu > 0$.

In addition, F_c is the radial collective force satisfying Eq. (3). The constant $Q = (\sigma_R - \sigma_L)\sigma_L I_0/c$ is associated with the squared effective charge of the atoms, with c being the speed of light and I_0 the total intensity of the six laser beams, while σ_R and σ_L represent the emission and absorption cross sections respectively. More precisely [34], the connection between Q and an effective charge q_{eff} is given by $Q = q_{eff}^2/\epsilon_0$, where ϵ_0 is the vacuum permittivity. The collective force is a contribution of two parts, the first one being the gradient of the incident laser intensity which gives rise an attractive force. This attractive force arises from in the imbalance of absorption of the light, since the intensities of the backward and forward are locally different. The second contribution is a repulsion force due the radiation pressure of scattered photons on nearby atoms. Light rescattering between atoms produces a repulsive interaction as a photon scattered from one atom tends to push away nearby atoms

[2]. In typical experiments [21] the repulsion dominates over the attractive force ($Q > 0$).

For the sake of definiteness we assume a polytropic equation of state $P = n_0 k_B T (n/n_0)^\gamma$, where γ is a generic polytropic index, n_0 is a reference number density and $k_B T$ is a reference thermal energy, where k_B is the Boltzmann constant. For definiteness, we restrict to $\gamma \geq 1$.

From a more fundamental point of view, collective phenomena in cold gases can be treated by means of kinetic theory, in terms of the Fokker-Planck equation for the probability distribution function. As described in [35], the diffusive term in the Fokker-Planck equation can be neglected provided the laser light is so intense so that the effects of absorption and radiation trapping forces dominate over photon exchange with the cooling laser. In this situation, the kinetic equation reduces to the Vlasov equation. Taking moments of the distribution function, one arrives to hydrodynamic equations for the macroscopic quantities, which can be closed assuming an equation of state [16–18, 35]. The drawback of the hydrodynamic approach is the loss of detailed information which is needed for kinetic effects such as Landau damping and kinetic instabilities. On the other hand, the treatment of nonlinear structures can be simpler within fluid models. We also remark that, below the critical temperature, the atomic boson gas presents a phase transition, so that both normal and condensed phases coexist. In this case a mean field theory for the condensed phase could be set up e. g. in terms of the Gross-Pitaevskii equation for the macroscopic condensate wave function [36]. However, the present work focuses on the nonlinear dynamics of the trapped cold gas, which is in a previous step towards Bose-Einstein condensation.

In order to derive arbitrary-amplitude solutions for the system (1)-(3), we introduce Lagrangian coordinates (ξ, τ), given [22–24] by

$$\xi = r - \int_0^\tau v(\xi, \tau')\, d\tau' \,, \quad \tau = t \,, \tag{5}$$

such that

$$\frac{\partial}{\partial \tau} = \frac{\partial}{\partial t} + v\,\frac{\partial}{\partial r} \,, \quad \frac{\partial}{\partial \xi} = \left(1 + \int_0^\tau \frac{\partial}{\partial \xi} v(\xi, \tau')\, d\tau'\right) \frac{\partial}{\partial r} \,. \tag{6}$$

The continuity equation (1) is then converted into

$$\frac{\partial}{\partial \tau}\left[\left(1 + \int_0^\tau \frac{\partial}{\partial \xi} v(\xi, \tau') d\tau'\right)\left(\xi + \int_0^\tau v(\xi, \tau') d\tau'\right)^2 n\right] = 0 \,, \tag{7}$$

with solution

$$n(\xi, \tau) = \frac{n(\xi, 0)\xi^2}{(1 + \int_0^\tau \frac{\partial}{\partial \xi} v(\xi, \tau') d\tau')(\xi + \int_0^\tau v(\xi, \tau') d\tau')^2} \,, \tag{8}$$

where $n(\xi,0)$ is the atomic cloud number density at $\tau=0$.

The Gauss law Eq. (3) in transformed coordinates is

$$\frac{\partial}{\partial\xi}\left[\left(\xi+\int_0^\tau v(\xi,\tau')d\tau'\right)^2 F_c\right] = Qn(\xi,0)\xi^2\,. \tag{9}$$

After solving Eq. (9) for F_c, the only remaining equation to be solved is the momentum transport Eq. (2), which becomes

$$\begin{aligned}\frac{\partial v}{\partial\tau} = &-\frac{\gamma k_B T}{m}\left(1+\int_0^\tau \frac{\partial}{\partial\xi}v(\xi,\tau')d\tau'\right)^{-1}\left(\frac{n}{n_0}\right)^{\gamma-2}\frac{\partial}{\partial\xi}\left(\frac{n}{n_0}\right) - \omega^2\left(\xi+\int_0^\tau v(\xi,\tau')d\tau'\right) - \nu v\\ &+\frac{\omega_p^2\int_0^\xi n(\xi',0)\xi'^2 d\xi'}{n_0(\xi+\int_0^\tau v(\xi,\tau')d\tau')^2}\,.\end{aligned} \tag{10}$$

where $\omega_p=(n_0 Q/m)^{1/2}$ is the plasma frequency for a reference number density n_0.

There are two manifest repulsion terms in Eq. (10). One of them is the pressure term proportional to $k_B T$ and the another one is due to the collective force, proportional to ω_p^2/n_0. These repulsion effects are counterbalanced by the $\sim\omega^2$ in the right-hand side of Eq. (10), which provides the confinement.

Equation (10) can be simplified if we suppose a linear velocity field

$$v=\dot{\rho}\xi\,, \tag{11}$$

where $\rho=\rho(\tau)$ is at this stage an arbitrary function, and where a dot denotes derivative with respect to τ. Without loss of generality, we set $\rho(0)=1$. Incidentally, the choice gives $\xi=r/\rho(\tau)$. Moreover, from Eq. (9) we get

$$\frac{\partial}{\partial\xi}(\xi^2 F_c) = \frac{Qn(\xi,0)\xi^2}{\rho^2}\,, \tag{12}$$

solved to

$$F_c=\frac{Q}{\rho^2\xi^2}\int_0^\xi n(\xi',0)\xi'^2 d\xi'\,, \tag{13}$$

with $F_c(0,\tau)=0$. To avoid singularities, we must enforce $\rho(\tau)>0$.

Inserting Eq. (11) into Eq. (8), we get

$$n=\frac{n(\xi,0)}{\rho(\tau)^3}\,. \tag{14}$$

It is also useful to have an expression of the total number N of confined atoms, which is

$$N=4\pi\int_0^\infty n(\xi,0)\xi^2 d\xi\,. \tag{15}$$

Inserting v from Eq. (11) and n from Eq. (14) into Eq. (10), the result is

$$(\ddot{\rho}+\nu\dot{\rho}+\omega^2\rho)\rho^{3\gamma-2} = -\frac{\gamma k_B T}{m\xi}\left(\frac{n(\xi,0)}{n_0}\right)^{\gamma-2}\frac{d}{d\xi}\left(\frac{n(\xi,0)}{n_0}\right) + \frac{\omega_p^2}{n_0}\frac{\rho^{3\gamma-4}\int_0^\xi n(\xi',0)\xi'^2 d\xi'}{\xi^3}\,. \quad (16)$$

The left-hand side of Eq. (16) is a function of τ only, while on the right-hand side the first term is a function of ξ only and the second term is a separable function of both variables. Deriving all terms in Eq. (16) once with respect to ξ and once with respect to τ gives

$$\omega_p^2\frac{d}{d\tau}(\rho^{3\gamma-4})\frac{d}{d\xi}\left(\frac{\int_0^\xi n(\xi',0)\xi'^2 d\xi'}{\xi^3}\right) = 0\,. \quad (17)$$

When the collective force can not be neglected, this gives restrictive conditions, namely: either $\gamma = 4/3$ (for non-constant ρ), or the term on the second bracket of Eq. (17) must be a constant, implying a constant $n(\xi,0)$. Hence, restricting to the more interesting situation where neither $\rho(\tau)$ nor $n(\xi,0)$ are constants, there are only three possibilities: (a) in the TL case where the $\sim \omega_p^2$ term can be neglected compared to the pressure term, the left-hand side of Eq. (16) should be balanced by the first term on the right-hand side therein. In this situation Eq. (17) is irrelevant; (b) in the MS case where the pressure term can be neglected, the left-hand side of Eq. (16) should be balanced by the $\sim \omega_p^2$ term; (c) if $\gamma = 4/3$, the whole right-hand side of Eq. (16) becomes a function of ξ only. In this situation both temperature and collective force effects can be maintained. The three possibilities will be analyzed in separate.

A. Temperature-limited (TL) regime

Disregarding the collective force shows that both the left and right-hand sides of Eq. (16) must be a constant, or

$$(\ddot{\rho}+\nu\dot{\rho}+\omega^2\rho)\rho^{3\gamma-2} = -\frac{\gamma k_B T}{m\xi}\left(\frac{n(\xi,0)}{n_0}\right)^{\gamma-2}\frac{d}{d\xi}\left(\frac{n(\xi,0)}{n_0}\right) = \omega_{TL}^2\,, \quad (18)$$

so that

$$\frac{d^2\rho}{d\tau^2} + \nu\frac{d\rho}{d\tau} + \omega^2\rho = \frac{\omega_{TL}^2}{\rho^{3\gamma-2}}\,, \quad (19)$$

where $\omega_{TL}^2 > 0$ is a constant taken as positive to avoid $\rho = 0$ in a finite time. By inspection it is possible to identify the general equilibrium solution $\rho = \rho_{\rm eq}$, wherein $\dot{\rho} = \ddot{\rho} = 0$, given by

$$\rho_{eq} = \left(\frac{\omega_{TL}^2}{\omega^2}\right)^{\frac{1}{3\gamma-1}}\,. \quad (20)$$

The spatial part of Eq. (18) separates into two classes, according to the value of γ.

Case I: $\gamma > 1$

When $\gamma > 1$, setting $\omega_{TL}^2 = 2\gamma k_B T/[m(\gamma-1)\xi_0^2]$ gives from Eq. (18),

$$n(\xi,0) = n_0 \left(1 - \left(\frac{\xi}{\xi_0}\right)^2\right)^{\frac{1}{\gamma-1}}, \quad \xi \leq \xi_0\,, \tag{21}$$

where ξ_0 is a reference length. For $\xi \geq \xi_0$ we set $n(\xi,0) = 0$. Since the more interesting physics takes place inside the atomic cloud, we will mainly discuss the problem restricted to $\xi \leq \xi_0$. We have assumed $n(0,0) = n_0$, which is the definition of n_0. From Eqs. (15) and (21), we get

$$N = n_0\,(\sqrt{\pi}\,\xi_0)^3\,\frac{\Gamma\left(\frac{\gamma}{\gamma-1}\right)}{\Gamma\left(\frac{5\gamma-3}{2(\gamma-1)}\right)}\,, \tag{22}$$

where Γ is the Gamma function. Equation (22) can be viewed as a tool to determine the cutoff ξ_0, given the total number of particles, the number density at $\xi = 0$ and the polytropic index.

For the sake of illustration, we set $\gamma = 5/3$, which corresponds to the usual tridimensional adiabatic coefficient. In this case, the Eq. (19) reads

$$\frac{d^2\rho}{d\tau^2} + \nu\frac{d\rho}{d\tau} + \omega^2\rho = \frac{\omega_{TL}^2}{\rho^3}\,, \tag{23}$$

which is an autonomous Pinney equation [37] with a damping term, where $\omega_{TL}^2 = 5k_BT/m\xi_0^2$. The Pinney equation is endemic in applied mathematics, appearing in cosmology [38, 39], magnetogasdynamics [40], quantum plasmas [41] Bose-Einstein condensates [42], dissipative quantum mechanics models [43] and many other contexts.

The undamped case ($\nu = 0$) was solved by Pinney [37], including a time-dependent frequency $\omega = \omega(t)$, in terms of the linearly independent solutions of the associated Hill equation. Due to the Doppler cooling, the present model becomes a dissipative Pinney equation [44]. It happens that the damped Pinney Eq. (23) admits an accurate approximate solution, derived from Kuzmak-Luke perturbation theory [45, 46], which is an appropriate tool for weakly damped nonlinear oscillator problems [47]. From Eq. (26) of [44], the solution reads

$$\rho^2 = \rho_{\rm eq}^2 + 2A^2e^{-\nu\tau} + 2A\,e^{-\nu\tau/2}\left(\rho_{\rm eq}^2 + A^2e^{-\nu\tau}\right)^{1/2}\cos\left(2\omega(\tau-\tau_0)\right)\,, \tag{24}$$

where A, τ_0 are integration constants. As detailed in [44], a weak damping assumption, namely $\nu << \omega$, should be valid for the accuracy of Eq. (24). In the undamped case ($\nu = 0$), Eq. (24) shows an exact oscillatory solutions in the interval $I = \{\rho > 0 \,|\, \sqrt{\rho_{\rm eq}^2 + A^2} - |A| \leq \rho \leq \sqrt{\rho_{\rm eq}^2 + A^2} + |A|\}$, with the parameter $|A|$ playing the rôle of an initial amplitude. Moreover, since $\nu/\omega \ll 1$, during one oscillation period $\tau = \pi/\omega$ the quantity $|A| \exp(-\nu\tau/2)$ does not change very much and plays the rôle of a slowly varying time-dependent amplitude. Notice that from Eq. (20) one has that $\rho_{eq} = (5k_BT/m\omega^2\xi_0^2)^{\frac{1}{4}}$.

Also from Eq. (24) setting $\rho(0) = 1$ implies

$$\tau_0 = \frac{1}{2\omega} \arccos\left(\frac{1 - \rho_{\rm eq}^2 - 2A^2}{2\,A\,(\rho_{\rm eq}^2 + A^2)^{1/2}}\right), \tag{25}$$

making sense if and only if $A^2 \geq (1 - \rho_{\rm eq}^2)^2/4$, to avoid $\cos^2(2\omega\tau_0) > 1$, which can be shown to be equivalent to $\rho = 1 \in I$, as discussed in [26]. Besides, taking into account Eq. (25), the parameter A is obviously related to $\dot\rho(0)$, but in an awkward algebraic way we refrain to exhibit.

Taking typical [3, 20] parameters $|\Delta| = 2.5\Gamma$ where $\Gamma = 2\pi \times 6\,\mathrm{MHz}$, $k_L \sim 10^7\,\mathrm{m}^{-1}$, $s_{inc} = 0.1$, $m = 1.41 \times 10^{-25}\,\mathrm{kg}$ (rubidium), $|\nabla B| = 25\,\mathrm{G/cm}$, $k_BT = 5.4 \times 10^{-27}\,\mathrm{J}$ (Doppler temperature), $\xi_0 = 0.28\,\mathrm{mm}$, $\omega = 697\,\mathrm{rad/s}$, $\nu = 231\,\mathrm{s}^{-1}$, together with $\omega_{TL} = 1560\mathrm{s}^{-1}$ and $\rho_{eq} = 1.5$, we have the damped oscillations shown in Fig. 1. The numerical simulation of Eq. (23) and the approximate solution from Eq. (24) yield almost identical results in this case.

The number density in this case becomes

$$n(\xi, 0) = n_0\left(1 - \left(\frac{\xi}{\xi_0}\right)^2\right)^{\frac{3}{2}}, \quad \xi \leq \xi_0\,. \tag{26}$$

From Eq. (22) we have the number of confined atoms

$$N = 4\pi \int_0^{\xi_0} n(\xi, 0)\xi^2 d\xi = 1.23\, n_0\xi_0^3\,. \tag{27}$$

For the parameters of Fig. 1 and $n_0 = 10^{15}\,\mathrm{m}^{-3}$ we have $N = 2.7 \times 10^4$ atoms, in agreement with experiments reported in [3].

The existence of the (stable) equilibrium is due to the sign of the inverse cubic term, which in turn comes from the concavity of the number density in Eq. (26). Alternatively, one can write the conservative part of Eq. (23) in terms of a potential $V = V(\rho)$, or

$$\ddot\rho + \nu\dot\rho = -(1/m)dV/d\rho\,, \quad V = \frac{m\omega^2\rho^2}{2} + \frac{5k_BT}{2\xi_0^2}\frac{1}{\rho^2}\,. \tag{28}$$

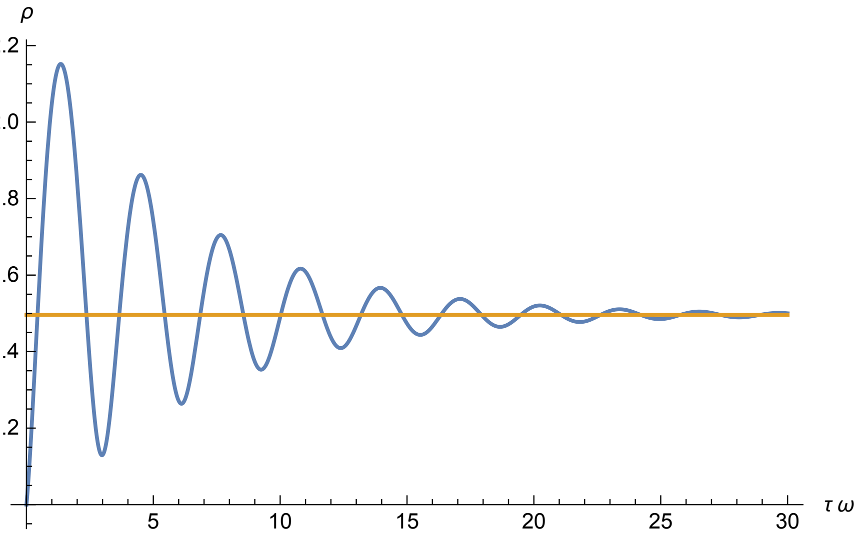

FIG. 1. Auxiliary function ρ as a function of time. Blue curve: analytical solution Eq. (24) with $A = 0.7$ and $\omega\tau_0 = 2.85$. Orange curve indicates $\rho_{eq} = 1.5$. Parameters: $m = 1.41 \times 10^{-25}\,$kg, $k_B T = 5.4 \times 10^{-27}\,$J, $\xi_0 = 0.28\,$mm, $\omega = 697\,$rad/s, $\nu = 231\,\mathrm{s}^{-1}$ and $\omega_{TL} = 1560\,\mathrm{s}^{-1}$. Initial conditions: $\rho(0) = 1$ and $\dot{\rho}(0) = 0$.

The repulsion term $\sim 1/\rho^2$ prevents collapse to the origin.

Using Eqs. (11) and Eq. (5) we can obtain the relation between the Lagrangian and the physical coordinates, namely $r = \xi\rho$ and $t = \tau$. Replacing Eqs. (21) and (24) into Eq. (14) we have that the number density in terms of physical coordinates is given by

$$n(r,t) = n_0 \frac{\left\{1 - r^2 \Big/ \left[\xi_0^2 \left(\rho_{\mathrm{eq}}^2 + 2A^2 e^{-\nu t} + 2A\, e^{-\nu t/2} \left(\rho_{\mathrm{eq}}^2 + A^2 e^{-\nu t}\right)^{1/2} \cos(2\omega(t-\tau_0))\right)\right]\right\}^{\frac{3}{2}}}{\left(\rho_{\mathrm{eq}}^2 + 2A^2 e^{-\nu t} + 2A\, e^{-\nu t/2} \left(\rho_{\mathrm{eq}}^2 + A^2 e^{-\nu t}\right)^{1/2} \cos\left(2\omega(t-\tau_0)\right)\right)^{\frac{3}{2}}}, \tag{29}$$

shown in Fig. 2.

In this subsection the collective force was neglected in comparison with the thermal effects. Nevertheless, the collective force F_c can be found from Eq. (13), evaluated in terms of hypergeometric functions for a density number given by Eq. (26) and general polytropic

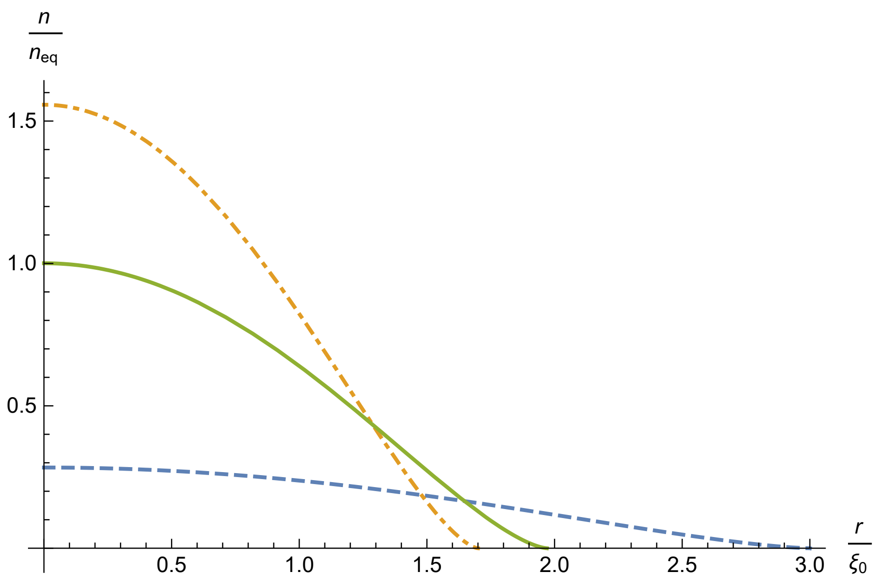

FIG. 2. Oscillations of the number density from Eq. (29), in the laboratory frame, normalized to the asymptotic value $n_{eq} = n_0/\rho_{eq}^3$. Dashed curve, blue: $\omega\tau = 4.5$; dash-dotted curve, orange: $\omega\tau = 15.5$; full curve, green: $\omega\tau = 30.5$.

coefficient. For $\gamma = 5/3$ we find

$$F_c = \frac{Qn_0\xi_0}{48\rho^2}\left(\frac{\xi_0}{\xi}\right)\left\{\left[1-\left(\frac{\xi}{\xi_0}\right)^2\right]^{\frac{1}{2}}\left[-8\left(\frac{\xi}{\xi_0}\right)^4+14\left(\frac{\xi}{\xi_0}\right)^2-3\right]+ + 3\frac{\arcsin(\xi/\xi_0)}{\xi/\xi_0}\right\}, \quad \xi \leq \xi_0\,, \tag{30}$$

shown in Fig. 3.

An alternative approach would be the linearization of the model around the equilibrium $n = 3m\omega^2/Q, v = 0, F_c = m\omega^2 r$. This method allows the derivation of plasma-like hybrid waves and modified Tonks-Dattner resonances [16–18], considering small amplitude perturbations. In comparison, the present Lagrangian variables technique allows the derivation of arbitrary amplitude analytical solutions, as apparent e.g. from Eqs. (29) and (30). In addition, the nonlinear dynamics of the modulating field ρ is also accessed, both from Kuzmak-Luke expansion and the identification of the potential $V(\rho)$ in Eq. (28), which shows the nonlinear stability of temporal oscillations. Similar remarks apply to all remaining nonlinear solutions below.

Case II: $\gamma = 1$

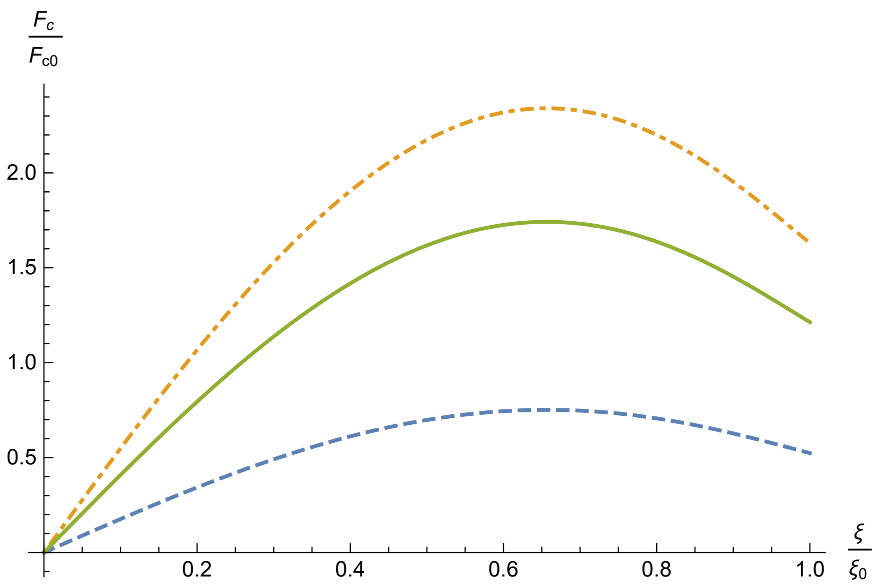

FIG. 3. Oscillations of the collective force inside of the atomic cloud, from Eq. (30) and normalized to $F_{c0} = Qn_0\xi_0/48$. Dashed curve, blue: $\omega\tau = 4.5$; dash-dotted curve, orange: $\omega\tau = 15.5$; full curve, green: $\omega\tau = 30.5$.

In the isothermal $\gamma = 1$ case we define $\omega_{TL}^2 = 2k_BT/(m\xi_0^2)$, so that Eq. (19) becomes

$$\frac{d^2\rho}{d\tau^2} + \nu\frac{d\rho}{d\tau} + \omega^2\rho = \frac{\omega_{TL}^2}{\rho}\,, \tag{31}$$

which describes a dissipative nonlinear anharmonic oscillator with an inverse linear force. Although a perturbative solution can be also found for small damping, it is too cumbersome to be of any help. The number density from Eq. (18) is

$$n(\xi, 0) = n_0 \exp\left(-\left(\frac{\xi}{\xi_0}\right)^2\right), \tag{32}$$

which has no cutoff. One can write the conservative part of Eq. (31) in terms of a potential $V = V(\rho)$, or

$$\ddot{\rho} + \nu\dot{\rho} = -(1/m)dV/d\rho\,, \quad V = \frac{m\omega^2\rho^2}{2} - \frac{2k_BT}{m\xi_0^2}\ln\rho\,. \tag{33}$$

The repulsion term shown in Eq. (33) prevents $\rho = 0$ in a finite time, as illustrated in Fig. 4. The equilibrium is $\rho_{eq} = [2k_BT/(m\omega^2\xi_0^2)]^{1/2}$.

The collective force is found from Eqs. (12) and (32),

$$F_c = \frac{Qn_0\xi_0}{4\rho^2}\left(\frac{\xi_0}{\xi}\right)^2\left[\sqrt{\pi}\,\mathrm{Erf}\left(\frac{\xi}{\xi_0}\right) - 2\frac{\xi}{\xi_0}\exp\left(-\frac{\xi^2}{\xi_0^2}\right)\right], \tag{34}$$

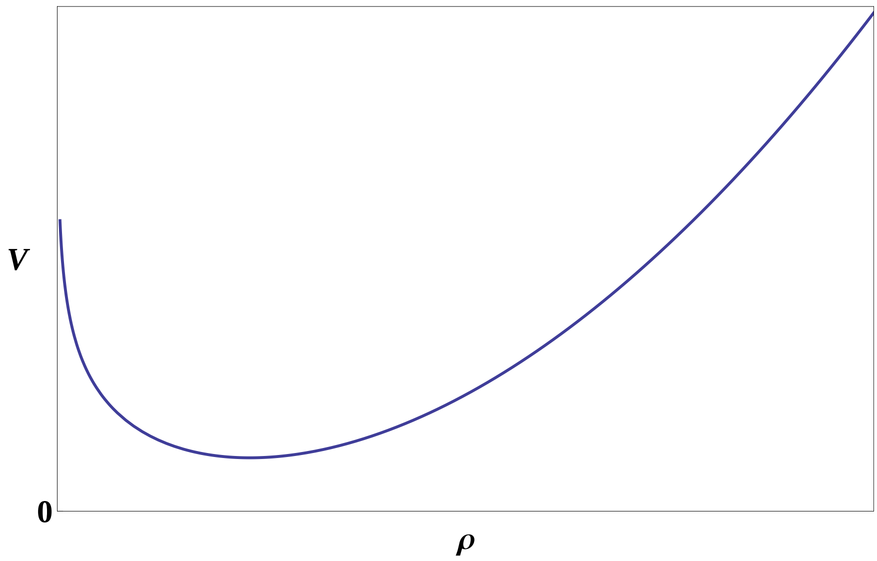

FIG. 4. Generic form of the potential in Eq (33), using arbitrary units.

shown in Fig. 5, where $\mathrm{Erf(s)} = (2/\pi^{\frac{1}{2}}) \int_0^{\mathrm{s}} \exp(-\mathrm{s}'^2)\mathrm{ds}'$ denotes the error function of generic argument s. Finally, from Eqs. (15) and (32) we have $N = n_0(\sqrt{\pi}\xi_0)^3$ confined atoms.

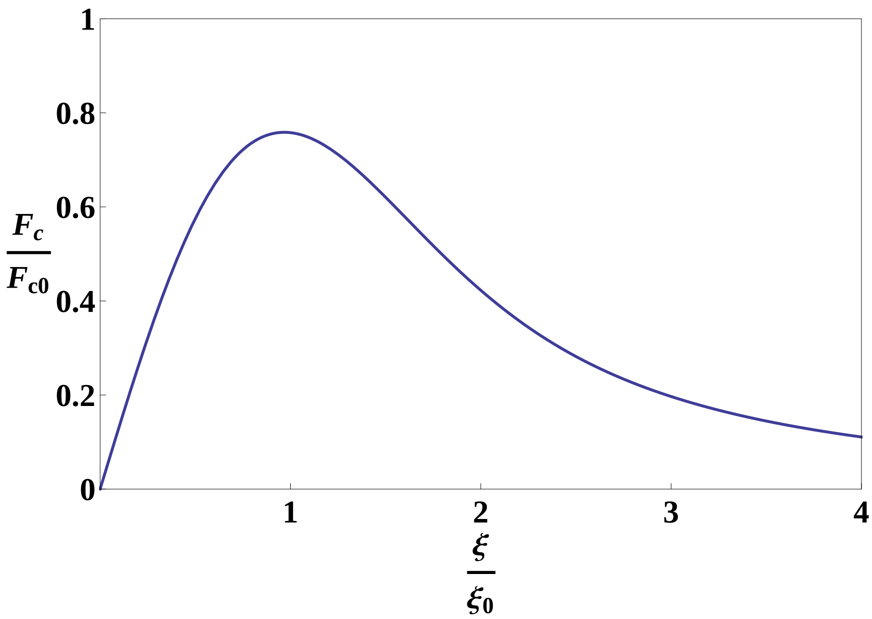

FIG. 5. Collective force from Eq. (34) for a fixed time, normalized to $F_{c0} = Qn_0\xi_0/(4\rho^2)$.

B. Multiple-scattering (MS) regime

When multiple-scattering dominates the pressure effects, one can drop the $\sim k_B T$ term in Eq. (16),

$$\left(\ddot{\rho}+\nu\dot{\rho}+\omega^2\rho\right)\rho^2=\frac{\omega_p^2\int_0^\xi \xi'^2 n(\xi',0)d\xi'}{n_0\xi^3}\,. \tag{35}$$

Focusing on a region inside the atomic cloud ($\xi<\xi_0$), the only way to satisfy Eq. (35) is to have an uniform density $n=n_0$ for $\xi<\xi_0$, where $\xi_0>0$ is a cutoff, while $n=0$ otherwise. Then Eq. (35) gives

$$\ddot{\rho}+\nu\dot{\rho}+\omega^2\rho=\frac{\omega_{MS}^2}{\rho^2}\,, \tag{36}$$

which describes a dissipative nonlinear oscillator, where $\omega_{MS}=\omega_p/\sqrt{3}$ is identical to the Mie oscillations frequency, in this case associated to the nonlinear contribution arising from the MS effects. By inspection it is possible to identify the general equilibrium solution, given by

$$\rho_{eq}=\left(\frac{\omega_{MS}^2}{\omega^2}\right)^{\frac{1}{3}}\,. \tag{37}$$

Alternatively, one can write the conservative part of Eq. (36) in terms of a potential $V=V(\rho)$,

$$\ddot{\rho}+\nu\dot{\rho}=-(1/m)dV/d\rho\,,\quad V=\frac{m\omega^2\rho^2}{2}+\frac{m\omega_{MS}^2}{\rho}\,. \tag{38}$$

As in the TL case, the damped oscillations of ρ never produce a singularity ($\rho=0$) in a finite time, thanks to the repulsion term in V. The undamped case ($\nu=0$) can be solved by quadratures in terms of elliptic functions.

In experiments with rubidium in the high density regime [1, 21, 30, 48], $n_0=10^{16}\,\mathrm{m}^{-3}$, the plasma frequency is typically $\omega_p\approx 200\,\mathrm{rad/s}$. For instance, if $\omega=697\,\mathrm{rad/s}$ and $\nu=231\,\mathrm{s}^{-1}$, then $\rho_{eq}=0.01$. With $\xi_0=1.8\,\mathrm{mm}$, the number of confined atoms is $N=(4\pi/3)n_0\xi_0^3=2.3\times10^8$, in agreement with [30].

Inside the atomic cloud ($r<\rho\xi_0$), the number density and the collective force are given by

$$n=\frac{n_0}{\rho^3}\,,\quad F_c=\frac{Qn_0 r}{3\rho^3}\,. \tag{39}$$

Asymptotically, in agreement with the literature [27, 30, 31, 48], $\rho\to\rho_{eq}$, so that $n\to n_{MS}\equiv 3n_0\omega^2/\omega_p^2=3kc/[(\sigma_R-\sigma_L)I_0\sigma_L]$, where k is the spring constant. As expected a stronger confinement $\sim\omega^2$ and a smaller collective force $\sim\omega_p^2$ produce a bigger number density.

C. Mixed TL + MS regime ($\gamma = 4/3$)

The restrictive condition in Eq. (17) is also satisfied for $\gamma = 4/3$, which allows to keep both thermal and collective effects. This polytropic index is an intermediate case between isothermal ($\gamma = 1$) and adiabatic ($\gamma = 5/3$) values. Equation (16) splits into

$$\frac{d^2\rho}{d\tau^2} + \nu\frac{d\rho}{d\tau} + \omega^2\rho = \frac{\Omega^2}{\rho^2} \tag{40}$$

and

$$-\frac{4k_BT}{m\xi}\frac{d}{d\xi}\left[\left(\frac{n(\xi,0)}{n_0}\right)^{1/3}\right] + \frac{\omega_p^2}{n_0\xi^3}\int_0^\xi n(\xi',0)\xi'^2 d\xi' = \Omega^2\,, \tag{41}$$

where $\Omega^2 > 0$ is a constant taken as positive to avoid $\rho = 0$ in a finite time.

The temporal part of the dynamics can be also written as

$$\ddot{\rho} + \nu\dot{\rho} = -(1/m)dV/d\rho\,, \quad V = \frac{m\omega^2\rho^2}{2} + \frac{m\Omega^2}{\rho}\,. \tag{42}$$

The equilibrium solution is $\rho_{eq} = (\Omega/\omega)^{2/3}$.

The spatial part described by Eq. (41) can be rewritten as

$$\frac{4}{R^2}\frac{d}{dR}\left(R^2\frac{d\bar{n}}{dR}\right) = \bar{n}^3 - 3\frac{\Omega^2}{\omega_p^2}\,, \tag{43}$$

where $\bar{n} = (n(\xi,0)/n_0)^{\frac{1}{3}}$ and $R = \xi/\lambda$ with $\lambda = [k_BT/(m\omega_p^2)]^{1/2}$ being the Debye length. The initial condition from the definition of $\bar{n}$ and from Eq. (41) should be $\bar{n}(0) = 1, \bar{n}'(0) = 0$, a prime denoting derivative with respect to R. Indeed, expanding in the vicinity of origin, Eq. (41) gives

$$4\frac{d\bar{n}}{dR} = (\bar{n}^3 - \frac{\Omega^2}{\omega_p^2})\,R + \mathcal{O}(R^2)\,, \tag{44}$$

so that $\bar{n}'(0) = 0$. If the nonlinear term $\sim \bar{n}^3$ could be discarded, Eq. (43) would be a Lane-Emden equation of index zero [49], which is exactly solvable. However, keeping all terms Eq. (43) needs to be numerically solved.

The parameter Ω^2 is related to the confinement characteristics. It is numerically verified that for $\Omega^2 > \omega_p^2/3$ one has only localized solutions $\bar{n}(R)$ for Eq. (43), with a cutoff $R_0 > 0$ such that $\bar{n}(R_0) = 0$. For $\Omega^2 < \omega_p^2/3$, the solution is unbound. Finally, if $\Omega = \omega_p/\sqrt{3}$ (the Mie oscillations frequency), the initial condition is a (linearly unstable) fixed point. The trapping occurring for Ω larger than the Mie frequency can be understood since from Eq.

(43) it corresponds to the initial condition as a maximum ($\bar{n}''(0) < 0$ for $\bar{n}(0) = 1, \bar{n}'(0) = 0$) of the number density. From now on we assume $\Omega > \omega_p/\sqrt{3}$.

Using Eq. (15) we find the number of trapped atoms,

$$N = 4\pi n_0 \lambda^3 \int_0^{R_0} \bar{n}^3(R) R^2 dR \,. \tag{45}$$

For a prescribed Ω/ω_p, one can find the cutoff R_0 from Eq. (43) together with $\bar{n}(0) = 1, \bar{n}'(0) = 0$. Then Eq. (45) gives the number of particles. Reciprocally, the inverse path provides Ω/ω_p as a function of N, which is the ultimate method for the determination of the otherwise undefined value of Ω given the remaining parameters (plasma frequency and Debye length).

Figure 6 shows the simulations result for Eq. (43) for two different values of $\eta = \Omega^2/\omega_p^2$. As expected, a larger η corresponds to a smaller R_0. For $\eta = 1$, we have from Eq. (45) that $R_0 = 3.09$ and $N = 5.16\,g$, where $g = 4\pi n_0 \lambda^3/3$ is the number of particles in a Debye sphere, while for $\eta = 2$ we have $R_0 = 0.49$ and $N = 1.47g$. For typical parameters $k_B T = 4.2 \times 10^{-27}\,\mathrm{J}$, $n_0 = 10^{16}\,\mathrm{m}^{-3}$, $m = 1.41 \times 10^{-25}\,\mathrm{m}^{-3}$ and $Q \sim 10^{-36}\,\mathrm{Nm}^2$ [1, 21] we then have $N = 1.8 \times 10^7$ (for $\eta = 1$) or $N = 5.1 \times 10^6$ (for $\eta = 2$) confined atoms. The general functional dependence of the cutoff R_0 in terms of η is shown in Fig. 7. As anticipated, confinement occurs for $\eta > 1/3$. Similarly, the numerical integration of Eq. (43) and applying Eq. (45) we have the number of confined atoms in terms of η, shown in Fig. 8.

III. Validity conditions

It is necessary to have a more detailed account on the validity conditions of the solution in the diverse regimes. This issue will be discussed in the immediate continuation.

A. Weak damping condition

In the dissipative Pinney equation Eq. (23), the approximate solution given by Eq. (24) holds with the condition $\nu \ll \omega$. Regarding Eqs. (4), the weak damping condition becomes

$$\frac{\mu_B |\nabla B| [m\Gamma(1 + 4\Delta^2/\Gamma^2)^2]}{8\hbar^2 k_L^3 s_{\mathrm{inc}} |\Delta|} \gg 1 \,. \tag{46}$$

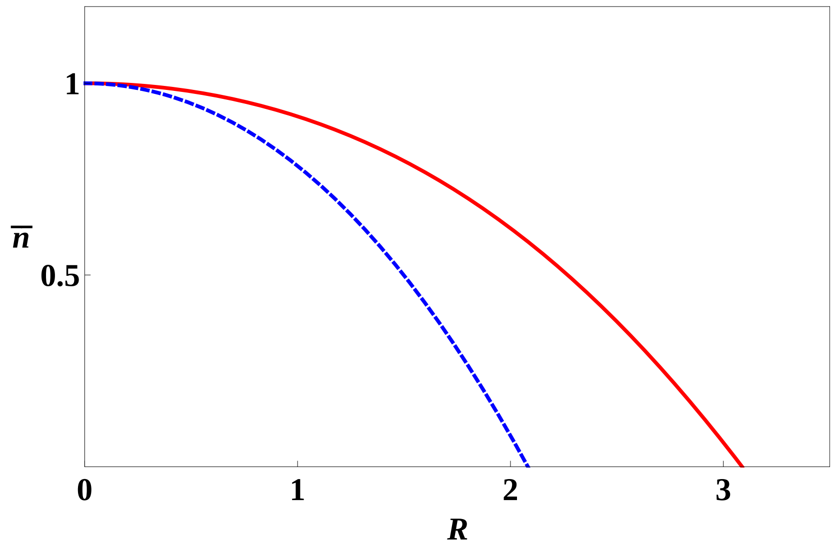

FIG. 6. Numerical solution of Eq. (43) with $\bar{n}(0) = 1, \bar{n}'(0) = 0$, for different values of $\eta = \Omega^2/\omega_p^2$. Upper curve, line, red: $\eta = 1$. Lower curve, dashed, blue: $\eta = 2$.

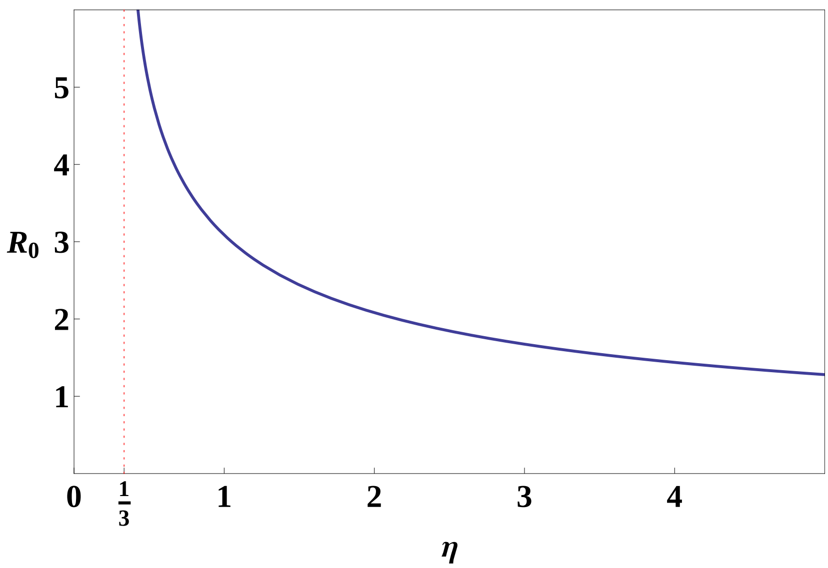

FIG. 7. Cutoff R_0 for the bound solutions of Eq. (43) as a function of the parameter $\eta = \Omega^2/\omega_p^2$.

In typical experiments $|\Delta| = 2.5\Gamma$ where $\Gamma = 2\pi \times 6\,\mathrm{MHz}$, $k_L \sim 10^7\,\mathrm{m}^{-1}$, $s_{inc} = 0.1$ and $m = 1.41 \times 10^{-25}\,\mathrm{kg}$. The weak damping conditions is satisfied for $|\nabla B| \gg 2.7\,\mathrm{G/cm}$, which is easily obtained since in MOTs the characteristic intensity of the gradient field is $|\nabla B| \geq 10\,\mathrm{G/cm}$ [3, 30, 32, 50].

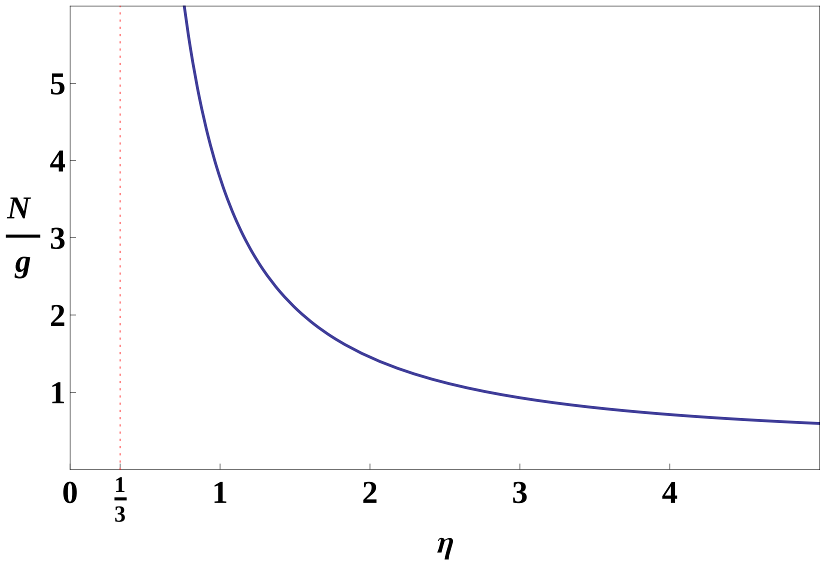

FIG. 8. Number N of confined atoms, normalized to the number of particles in a Debye sphere $g = 4\pi n_0 \lambda^3/3$, as a function of the parameter $\eta = \Omega^2/\omega_p^2$. From Eq. (45) and after numerical integration of Eq. (43).

B. TL regime: validity conditions

We can analytically evaluate the pressure dominance condition of II.A in the specific case $\gamma = 5/3$. From comparison of the repulsion terms in Eq. (16) and using Eq. (26), it amounts to $5k_BT\xi/(m\xi_0^2) \gg F_c/m$, where the collective force is given by Eq. (30). Some algebra then yields

$$\frac{15k_BT}{m\omega_p^2\xi_0^2} >> \rho f(\xi/\xi_0)\,, \tag{47}$$

where

$$f(\xi/\xi_0) = \frac{1}{16}\left(\frac{\xi_0}{\xi}\right)^2\left\{\left[1-\left(\frac{\xi}{\xi_0}\right)^2\right]^{\frac{1}{2}}\left[-8\left(\frac{\xi}{\xi_0}\right)^4+14\left(\frac{\xi}{\xi_0}\right)^2-3\right]+3\frac{\arcsin(\xi/\xi_0)}{\xi/\xi_0}\right\} \leq 1\,. \tag{48}$$

The last estimate happens because $f(\xi/\xi_0) \leq 1$ as seen in Fig. 9.

The most stringent constraint from the inequality in Eq. (47) is for the maximum value $\rho = \rho_{\rm max} \approx \sqrt{\rho_{\rm eq}^2 + A^2} + |A|$, a return point obtained from the perturbative solution (24) where damping was neglected, for the sake of the estimate. Hence, the pressure dominance assumption holds for

$$\frac{15k_BT}{m\omega_p^2\xi_0^2} \gg \sqrt{\rho_{\rm eq}^2 + A^2} + |A| \geq \frac{1}{2}(1 + \rho_{\rm eq}^2 + |1-\rho_{\rm eq}^2|)\,, \tag{49}$$

where the last inequality is due to the constraint reported below Eq. (25) in order to satisfy the initial condition $\rho(0) = 1$. In terms of the physical parameters, the inequality (49) unveils two subclasses, as follows.

1. *Thermal dominated equilibrium*

The thermal dominated equilibrium ($\rho_{\rm eq} = [5k_BT/(m\omega^2\xi_0^2)]^{1/4} \geq 1$) case corresponds to

$$\left(\frac{\sqrt{3}\,\omega}{\omega_p}\right)\rho_{eq}^2 \gg \rho_{eq} \geq 1\,. \tag{50}$$

Under the condition (50), one can neglect the collective force. It is interesting to note that the trap frequency ω is not necessarily bigger than the Mie frequency $\omega_p/\sqrt{3}$, provided that thermal effects are large enough so that $\rho_{eq} \gg 1$.

2. *Harmonic confinement dominated equilibrium*

Whenever the trap is strong enough so that $\rho_{eq} \leq 1$, Eq. (49) implies

$$1 \geq \rho_{eq}^2 \gg \frac{\omega_p}{\sqrt{3}\,\omega}\,, \tag{51}$$

which needs a large harmonic confinement frequency compared to the Mie oscillations frequency.

All in all, both Eqs. (50) and (51) show that

$$\rho_{eq}^2 \gg \frac{\omega_p}{\sqrt{3}\,\omega} \tag{52}$$

is the ultimate condition to rigorously justify the TL approximation, when $\gamma = 5/3$. For the parameters of Fig. 1 together with $n_0 = 10^{15}\,\mathrm{m}^{-3}$, $Q \sim 10^{-36}\,\mathrm{Nm}^2$ gives $\omega_p/\sqrt{3} = 48.6\,\mathrm{rad/s}$ while $\omega = 697\,\mathrm{rad/s}$. This example fits the thermal dominated scenario, with $\rho_{eq} = 1.5$.

On the other hand, proceeding as before but for the isothermal case $\gamma = 1$, we get

$$\frac{6k_BT}{m\omega_p^2\xi_0^2} >> \frac{h(\xi/\xi_0)}{\rho}\,, \tag{53}$$

where

$$h(\xi/\xi_0) = \frac{3}{4}\left(\frac{\xi_0}{\xi}\right)^3\left[\sqrt{\pi}\,\mathrm{Erf}\left(\frac{\xi}{\xi_0}\right) - 2\frac{\xi}{\xi_0}\exp\left(-\frac{\xi^2}{\xi_0^2}\right)\right] \leq 1\,. \tag{54}$$

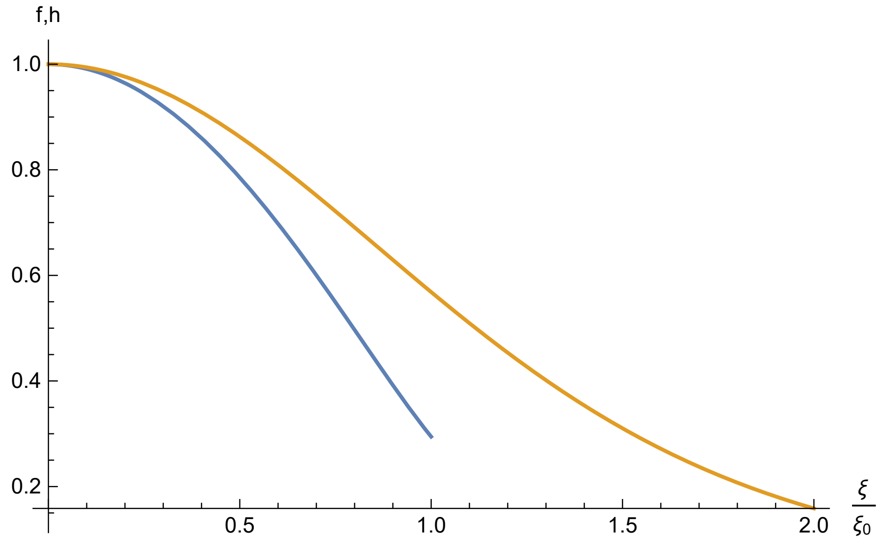

FIG. 9. Lower curve, blue: function $f(\xi/\xi_0)$ from Eq. (48); upper curve, orange: $h(\xi/\xi_0)$ from Eq. (54).

The function $h(\xi/\xi_0)$ is shown in Fig. 9.

The most stringent condition from Eq. (53) happens for $h(\xi/\xi_0) = 1$ and $\rho = \rho_{eq} = [2k_B T/(m\omega^2\xi_0^2)]^{1/2}$ which is the minimum of the potential V in Eq. (33). We then get

$$\rho_{eq} \gg \left(\frac{\omega_p}{\sqrt{3}\,\omega}\right)^{2/3} \tag{55}$$

as the condition for the TL regime in the isothermal case. This is similar to Eq. (52), keeping in mind the slightly different expressions for ρ_{eq} in the adiabatic $\gamma = 5/3$ and isothermal $\gamma = 1$ cases. Also, in terms of the number of particles,

$$N \ll n_{MS}\left(\frac{2\pi k_B T}{k}\right)^{\frac{3}{2}}\,, \tag{56}$$

which is in agreement with [3].

Reciprocally, the validity conditions for the MS regime are the inverse of the conditions for the TL regime.

IV. Conclusion

In this work, nonlinear, time-dependent structures were derived for trapped cold atoms in a magneto optical trap, in terms of the Lagrangian variables method. Three classes of solutions have been identified. The first class is for thermally dominated systems with an arbitrary polytropic coefficient, which for an adiabatic equation of state reduces to a damped Pinney equation (an endemic ordinary differential equation in nonlinear mechanics), with dissipative features due to the Doppler cooling. The second class of solutions is applicable to multiple-scattering dominated systems. The third class (with polytropic index $\gamma = 4/3$) of solutions is applicable when the joint TL and MS effects are relevant. In all cases, the solutions are valid for specific forms of the initial particle number density, while the time-evolution is given in terms of the damped nonlinear oscillations of the scale function ρ. The validity conditions for the solutions have been analytically determined in terms of the physical parameters, which can helps the experimental verification of the predictions. In this context the main advantage of the Lagrangian variables method is to provide a detailed analytical account of the non-stationary and nonlinear aspects of the dynamics, unavailable through other approaches. Also notice that the present approach can be directly adapted to non-neutral, confined plasmas, where the damping mechanism can be traced back to collisions with neutrals.

The spirit of this work can be generalized in several directions, like for more complex geometries due the misalignment of the lasers in xy-plane which gives rise a tangential force [31, 33], asymmetric forces, harmonic traps with a time-dependent frequency $\omega = \omega(t)$ and single-component, non-neutral plasmas. Finally, it would be interesting to characterize the linear limit of our derived nonlinear structures, potentially offering a more precise connection with previous treatments in the literature [16–18]. These possibilities are under investigation and will be reported elsewhere.

Acknowledgments: L. G. F. S. and F. H. acknowledge the support by Conselho Nacional de Desenvolvimento Científico e Tecnológico (CNPq). This study was financed in part by the Coordenação de Aperfeiçoamento de Pessoal de Nível Superior - Brasil (CAPES) - Finance Code 001.

[1] G. Labeyrie, F. Michaud and R. Kaiser, Phys. Rev. Lett. **96**, 023003 (2006).

[2] A. di Stefano, M. Fauquembergue, P. Verkerk and D. Hennequin, Phys. Rev. A **67**, 033404 (2003).

[3] C. G. Townsend, N. H. Edwards, C. J. Cooper, K. P. Zetie, C. J. Foot, A. M. Steane, P. Szriftgiser, H. Perrin and J. Dalibard, Phys. Rev. A **52**, 1423 (1995).

[4] T. Pohl, G. Labeyrie and R. Kaiser, Phys. Rev. A **74**, 023409 (2006).

[5] L. Guidoni and P. Verkerk, J. Opt. B: Quantum Semiclassical Opt. **1**, R23 (1999).

[6] I. Bloch, Nat. Phys. **1**, 23 (2005).

[7] M. H. Anderson, J. R. Ensher, M. R. Matthews, C. E. Wieman and E. A. Cornell, Science **269**, 198 (1995).

[8] S. Stellmer et al, Phys. Rev. Lett. **110**, 263003 (2013).

[9] K. Gibble and S. Chu, Phys. Rev. Lett. **70**, 1771 (1993)

[10] G. Santareli et al, Phys. Rev. Lett. **82**, 4619 (1999)

[11] G. Manfredi and P.-A. Hervieux, Phys. Rev. Lett. **109**, 255005 (2012).

[12] J. P. Cox, *Theory of stellar pulsation* (Princeton University Press, Princeton, 1980).

[13] D. Dreon, L. A. Sidorenkov, C. Bouazza, W. Maineult, J. Dalibard and S. Nascimbene, J. Phys. B: At. Mol. Opt. Phys. **50**, 065005 (2017).

[14] R. Ayllon, H. Terças and J. T. Mendonça, Phys. Plasmas **26**, 033501 (2019).

[15] B. B. Zelener, I. D. Arshinova, A. A. Bobrov, E. V. Vilshanskaya, S. A. Saakyan, V. A. Sautenkov, B. V. Zelener and V. E. Fortov, JETP Letters **108**, 820 (2018).

[16] H. Terças, R. Kaiser, J. T. Mendonça and J. Loureiro, Phys. Rev. A **78**, 013408 (2008).

[17] H. Terças, J. T. Mendonça and R. Kaiser, Europhys. Lett. **89**, 53001 (2010).

[18] H. Terças and J. T. Mendonça, Phys. Rev. A **88**, 023412 (2013).

[19] R. S. de Oliveira, E. P. Raposo and S. S. Vianna, Phys. Rev. A **70**, 023402 (2004).

[20] A. S. Arnold and P. J. Manson, J. Opt. Soc. Am. B **17**, 497 (2000).

[21] G. L. Gattobigio, F. Michaud, G. Labeyrie, T. Pohl and R. Kaiser, AIP Conf. Proc. **862**, 211 (2006).

[22] R. C. Davidson, *Methods in nonlinear plasma theory* (Academic Press, New York, 1972).

[23] E. Infeld and G. Rowlands, *Nonlinear waves, solitons and chaos* 2nd. ed. (Cambridge University Press, Cambridge, 2000).

[24] B. K. Shivamoggi, *Introduction to nonlinear fluid-plasma waves* (Kluwer, Dordrecht, 1988).

[25] S. Ghosh, N. Chakrabarty and F. Haas, Europhys. Lett. **105**, 30006 (2014).

[26] F. Haas and L. G. F. Soares, Phys. Plasmas **25**, 012310 (2018).

[27] A. M. Steane, M. Chowdhury and C. J. Foot, J. Opt. Soc. Am. B **9**, 2142 (1992).

[28] P. Kohns, P. Buch, W. Süptitz, C. Csambal and W. Ertmer, Europhys. Lett. **22**, 517 (1993).

[29] A. Fioretti, A. F. Molisch, J. H. Müller, P. Verkerk and M. Allegrini, Opt. Commun. **149**, 415 (1998).

[30] G. L. Gattobigio, T. Pohl, G. Labeyrie and R. Kaiser, Physica Scripta. **81**, 025301 (2010).

[31] D. W. Sesko, T. G. Walker and C. E. Wieman, J. Opt. Soc. Am. B **8**, 946 (1991).

[32] C. D. Wallace, T. P. Dinneen, K. Y. N. Tan, A. Kumarakrishnan, P. L. Gould and J. Javanainen, J. Opt. Soc. Am. B **11**, 703 (1994).

[33] I. Guedes, M. T. de Araujo, D. M. B. P. Milori, G. I. Surdutovich, V. S. Bagnato and S. C. Zilio, J. Opt. Soc. Am. B **11**, 1935 (1994).

[34] T. Walker, D. Sesko and C. Wieman, Phys. Rev. Lett. **64**, 408 (1990).

[35] L. Pruvost, I. Serre, H. T. Duong and J. Jortner, Phys. Rev. A **61**, 053408 (2000).

[36] C. J. Pethick and H. Smith, *Bose-Einstein condensation in dilute gases* (Cambridge University Press, Cambridge, 2008).

[37] E. Pinney, Proc. Amer. Math. Soc. **1**, 681 (1950).

[38] R. M. Hawkins and J. E. Lidsey, Phys. Rev. D **66**, 023523 (2002).

[39] H. C. Rosu, S. C. Mancas and P. Chen, Phys. Lett. A **379**, 882 (2015).

[40] C. Rogers and W. K. Schief, J. Math. Phys. **52**, 083701 (2011).

[41] F. Haas and A. Bret, Europhys. Lett. **97**, 26001 (2012).

[42] F. Haas, Phys. Rev. A **65**, 33603 (2002).

[43] F. Haas, J. M. F. Bassalo, D. G. da Silva, A. B. Nassar and M. Cattani, Int. J. Theor. Phys. **52**, 88 (2013).

[44] F. Haas, Physica Scripta **81**, 025004 (2010).

[45] G. E. Kuzmak, Pure Math. Manuscript **23**, 515 (1959).

[46] J. C. Luke, Proc. Roy. Soc. Ser. A **292**, 403 (1966).

[47] J. Kevorkian and J. D. Cole, *Perturbation methods in applied mathematics* (New York, Springer-Verlag, 1981).

[48] G. Labeyrie, G. L. Gattobigio, T. Pohl and R. Kaiser, AIP Conference Proceedings **970**, 303 (2008).

[49] S. Chandrasekhar, *An introduction to the study of stellar structure* (New York, Dover, 1967).

[50] K. Shibata, S. Yonekawa and S. Tojo, Phys. Rev. A **96**, 013402 (2017).